Magnetic phase diagram for a non-extensive system: Experimental connection with manganites

M.S. Reis^{*} and V.S. Amaral

Departamento de Física, Universidade de Aveiro, 3810-193 Aveiro, Portugal

J.P. Araújo

IFIMUP, Departamento de Física, Universidade do Porto, 4150 Porto, Portugal

I.S. Oliveira

Centro Brasileiro de Pesquisas Físicas, Rua Dr. Xavier Sigaud 150 Urca, 22290-180 Rio de Janeiro-RJ, Brazil (Dated: May 21, 2019)

In the present paper we make a thorough analysis of a classical spin system, within the framework of Tsallis nonextensive statistics. From the analysis of the generalized Gibbs free energy, within the mean-field approximation, a para-ferromagnetic phase diagram, which exhibits first and second order phase transitions, is built. The features of the generalized, and classical, magnetic moment are mainly determined by the values of q, the non-extensive parameter. The model is successfully applied to the case of $La_{0.60}Y_{0.07}Ca_{0.33}MnO_3$ manganite. The temperature and magnetic field dependence of the experimental magnetization on this manganite are faithfully reproduced. The agreement between rather "exotic" magnetic properties of manganites and the predictions of the q-statistics, comes to support our early claim that these materials are magnetically nonextensive objects.

PACS numbers:

I. INTRODUCTION

In the literature of manganites, various models have appeared as different attempts to reproduce the electric and magnetic properties of these systems. Krivoruchko et $al.^1$, Nunez-Regueiro et $al.^2$ and Dionne³ are interesting examples of multiparameter models, but which failed to achieve full agreement to experimental data. Ravindranath et $al.^4$ compare resistivity data in La_{0.6}Y_{0.1}Ca_{0.3}MnO₃ to different two-parameter models, which do not agree to each other in the low-temperature range. Other interesting attempts can be found in the work of Rivas et $al.^5$, Hueso et $al.^6$, Heremans et $al.^7$, Pal et $al.^8$, Philip et $al.^9$, Szewczyk et $al.^{10}$, Viret et $al.^{11}$ and Tkachuk et $al.^{12}$. None of these obtained plain agreement between experiment and theory, irrespect their number of adjusting parameters and approach.

On another hand, Tsallis generalized statistics^{13,14,15,16}, has been successfully applied to an impressive number of areas¹⁷. The formalism rests on the definition of generalized entropy¹³:

$$S_q = k \frac{1 - \sum_i p_i^q}{q - 1} \tag{1}$$

where q is the entropic index, p_i are probabilities satisfying $\sum_i p_i = 1$ and k is a positive constant. The above formula converges to the usual Maxwell-Boltzmann definition of entropy, and to the usual derived thermodynamic functions, in the limit $q \to 1^{13,14,15,16,17}$.

In what concerns Condensed Matter problems, applications of Eq.1 include: Ising ferromagnets^{18,19,20,21,22}, molecular field approximation^{23,24,25}, percolation problems²⁶, Landau diamagnetism^{27,28}, electron-phonon systems and tight-binding-like Hamiltonians^{29,30,31}, metallic³² and superconductor³³ systems, etc. The first evidences that the magnetic properties of manganites could be described within the framework of Tsallis statistics were presented by Reis *et al.*³⁴, followed by an analysis³⁵ of the unusual paramagnetic susceptibility of La_{0.67}Ca_{0.33}MnO₃, measured by Amaral *et al.*³⁶.

Maximization of Eq.1 subjected to the constraint of the normalized q-expectation value of the Hamiltonian $\hat{\mathcal{H}}^{14,15}$:

$$U_q = \frac{Tr\{\hat{\mathcal{H}}\hat{\rho}^q\}}{Tr\{\hat{\rho}^q\}} \tag{2}$$

and the usual normalization of the density matrix $Tr\{\hat{\rho}\} = 1$, yields the following expression for the density matrix $\hat{\rho}$:

$$\hat{\rho} = \frac{1}{Z_q} [1 - (1 - q)\tilde{\beta}(\hat{\mathcal{H}} - U_q)]^{1/(1 - q)}$$
(3)

where

$$Z_q = Tr[1 - (1 - q)\tilde{\beta}(\hat{\mathcal{H}} - U_q)]^{1/(1 - q)}$$
(4)

is the partition function and $\tilde{\beta} = \beta/Tr\{\hat{\rho}^q\}$. Here, β is the Lagrange parameter associated to the internal energy.

The magnetization of a specimen is, accordingly, given by 14,15,16,34,35 :

$$M_q = \frac{Tr\{\hat{\mu}\hat{\rho}^q\}}{Tr\{\hat{\rho}^q\}} \tag{5}$$

where $\hat{\mu}$ is the magnetic moment operator.

However, Eq.3 can be written in a more convenient form^{14,15,34,35} in terms of β^* , defined as $\beta^* = \tilde{\beta}/[1 + (1-q)\tilde{\beta}U_q]$. In particular, to analyze the physical system described here, the quantity $1/(k\beta^*)$ will represent the physical temperature scale, as in references^{34,35}. Discussion about the concept of temperature and Lagrange parameters in Tsallis statistics can be found in the literature^{14,15,34,35,37,38,39}. In the present work, the q parameter is restricted to the interval $0 \le q \le 1$, preserving the entropy concavity^{35,40}.

In this paper we pursue the idea, based on novel experimental and theoretical results, that manganites are magnetically non-extensive objects. This property appears in systems where long-range interactions and/or fractality exist, and such features have been invoked in recent models of manganites, as well as in the interpretation of experimental results. They appear, for instance, in the work of Dagotto and co-workers⁴¹, who emphasize the role of the competition between different phases to the physical properties of these materials. Various authors have considered the formation of micro-clusters of competing phases, with *fractal* shapes, randomly distributed in the material 42,43 , and the role of *long-range interactions* to phase segregation^{44,45}. Important experimental results in this direction have also been reported by Marithew et al.⁴⁶, and Fiebig et al.⁴⁷. Particularly insightful is the work of Satou and Yamanada⁴⁸, who derived a *Cantor* spectra for the double-exchange hamiltonian, basis of theoretical models of manganites.

A major difficulty with Tsallis formulation concerns the physical meaning of the entropic parameter q. In this direction, Beck and Cohen⁴⁹ have recently shown that the value of q gives a direct measure of the internal distribution of temperatures in an *inhomogeneous* system. Although their results are not directly applied to magnetic systems, it has been known for some time that manganites are magnetically inhomogeneous systems (see, for instance, Ref.^{41,50} and references therein), and this fact has been explored very recently by Salamon *et al.*⁵¹, who applied the idea of *distribution* of the inverse susceptibility (which turns out to be equivalent to a distribution of temperatures), to the analysis of the magnetic susceptibility and the effective paramagnetic moment of La_{0.7}Ca_{0.3}MnO₃.

In what follows, we present a magnetic model for classical spins (cluster), using for that, the Tsallis generalized statistic. In the model, we consider that non-extensivity exists in the intra-cluster interaction, whereas the intercluster interaction remains extensive. This is important to maintain the total magnetization proportional to the number of clusters. Following, the Gibbs free energy is analyzed, within the mean-field approximation, and a series of interesting magnetic features appears, as a consequence of the intra-cluster non-extensivity. Finally, a connection between the model proposed here and the experimental data obtained from magnetic measurements performed on manganites support our thesis that these objects are magnetically non-extensive.

II. CLASSICAL MODEL

Consider a classical spin $\vec{\mu}$ submitted to a homogeneous magnetic field \vec{H} . The hamiltonian \mathcal{H} is given by

$$\mathcal{H} = -\mu H \cos \theta \tag{6}$$

where θ is the angle between $\vec{\mu}$ and \vec{H} . Following the usual Tsallis formalism^{14,15,16,34,35}, the magnetization \mathcal{M}_q can be determined from Eq.5, yielding:

$$\frac{\mathcal{M}_q}{\mu} = \mathcal{L}_q(x) = \frac{1}{(2-q)} \begin{cases} 1 - \frac{1}{x}, & x > \frac{1}{1-q} \\ \coth_q(x) - \frac{1}{x}, & x < \frac{1}{1-q} \end{cases}$$
(7)

where $x = \mu H/kT$, and $coth_q$ is the generalized qhyperbolic co-tangent⁵². The above two branches function results from the Tsallis cut-off^{15,16,53,54}. It is interesting to note the similarity between the above result and the traditional Langevin function. In what follows, Eq.7 will be called *Generalized Langevin Function*, and this result can also be derived from the *Generalized Brillouin Function*, introduced in Ref.³⁵, taking the limit of large spin values $(S \to \infty)$. The result derived above is valid only for $0 \le q \le 1$.

The generalized magnetic susceptibility χ_q shows the usual dependence on the inverse of the absolute temperature

$$\chi_q = \lim_{H \to 0} \left[\frac{\partial \mathcal{M}_q}{\partial H} \right] = \frac{q\mu^2}{3kT} = q\chi_1 \tag{8}$$

and is proportional to the usual paramagnetic Langevin susceptibility χ_1 . A similar result was deduced for the generalized Brillouin function³⁵.

III. MEAN-FIELD APPROXIMATION

A. Gibbs Free Energy

The Gibbs free energy is, within the mean field approximation,

$$G = \frac{kT}{\mu} \int_0^{\mathcal{M}_q} \mathcal{M}_q^{-1}(\mathcal{M}_q') d\mathcal{M}_q' - H\mathcal{M}_q - \frac{\lambda}{2} \mathcal{M}_q^2 \qquad (9)$$

where the first term is the entropy, with \mathcal{M}_q^{-1} the inverse function of the generalized Langevin function (Eq.7); the second is the Zeeman term; and the third, the exchange energy, with λ as the mean field parameter. The equilibrium magnetization can be found from the minimization of the Gibbs free energy and, depending on the q value, first or second order transition features emerge. At zero magnetic field and for q>0.5 the free energy presents, at any temperature, only one minimum, for positive values of magnetization. Correspondingly, a second order paraferromagnetic phase transition occurs at $T_c^{(q)} = qT_c^{(1)}$, as sketched in figure 1(a). Here, $T_c^{(1)} = \mu^2 \lambda/3k$ is the Curie temperature for the standard Langevin model. From now on, we introduce the dimensionless temperature and field parameters $t = T/T_c^{(1)}$ and $h = \mu H/kT_c^{(1)}$.

For q < 0.5 the nature of the phase transition is more complex, presenting a typical behavior of first order phase transition⁵⁵. As it is illustrated in figure 1(b), for sufficiently high temperatures $(t > t_{SH})$, only one minimum at $\mathcal{M}_q = 0$ is observed. Decreasing temperature, at $t = t_{SH}$, a second minimum appears with finite magnetization and further lowering temperature to $t = t_c$, this minimum becomes degenerate, corresponding to $\mathcal{M}_q = 0$. For $t < t_c$ the free energy global minimum occurs for finite magnetization, determining its equilibrium value. However, this equilibrium state is not necessarily the one observed in finite times, since there is an energy barrier between the two minima, which prevent the whole system to reach the global minimum of energy. The minimum temperature that can sustain zero magnetization is the one corresponding to $t = t_{SC}$, where the energy barrier goes to zero and only one minimum exists at finite magnetization. In a similar way, t_{SH} corresponds to the maximum temperature that can sustain a finite magnetization. These phenomena are the wellknown 'superheating' and 'supercooling' cycles and are responsible for the thermal hysteresis normally observed in first order phase transitions⁵⁵. The t_{SH} and t_{SC} temperatures can be analytically derived from the conditions described above, and are valid only for $q \leq 0.5$, yielding:

$$t_{SH} = \frac{3}{4} \frac{1}{(2-q)} \tag{10}$$

$$t_{SC} = q \tag{11}$$

On the contrary, a closed expression for t_c cannot be derived, since it involves transcendental equations. The temperature dependence of the reduced equilibrium magnetization $\mathcal{M}_q(2-q)/\mu$ is sensitive to the features described above, as it can be seen in figure 2 and inset therein.

B. Magnetic Susceptibility

The generalized magnetic susceptibiliy χ_q , for any q value, can be derived from Eq.9,

$$\chi_q = \frac{C^{(q)}}{t - \theta_p^{(q)}} \tag{12}$$

where, in analogy with the usual Curie-Weiss law, we define

$$C^{(q)} = \frac{\mu}{kT_C^{(1)}} \left[\left. \frac{\partial \mathcal{M}_q^{-1}}{\partial \mathcal{M}_q} \right|_{\mathcal{M}_q(H=0,T)} \right]^{-1}$$
(13)

as the Generalized Curie Function. In the paramagnetic phase, $t \ge t_c$, M(H = 0, T) = 0 and the functions $C^{(q)}$ and $\theta_p^{(q)} = \lambda C^{(q)}$ are constants:

$$C^{(q)} = \frac{q}{\lambda} \tag{14}$$

$$\theta_p^{(q)} = q \tag{15}$$

The temperature dependence of χ_q , and its inverse, are quite distinct, depending whether q < 0.5 or q > 0.5, as displayed in figure 3(a) and (b), respectively. For q > 0.5the susceptibility diverges at t_c , the same temperature where its inverse intercepts the temperature axis at $\theta_p^{(q)}$. For q < 0.5 the susceptibility is always finite and peaks discontinuously at t_c . Correspondingly, its inverse shows a discontinuity with finite values and the Curie-Weiss linear behavior extrapolates to $\theta_p^{(q)}$, which is lower than t_c .

C. Influence of Magnetic Field on the Phase Transition

From the analysis of the Gibbs free energy, we conclude that for q < 0.5 and h = 0, the equilibrium magnetization has a first order phase transition. Sufficiently high magnetic field $h \ge h_{0q}$, is able to remove the energy barrier between the two minima in the Gibbs free energy and, consequently, the discontinuity in the equilibrium magnetization curve. This effect is illustrated in figure 4. The expression for h_{0q} can be derived from the condition described above, yielding:

$$h_{0q} = \frac{3(1-2q)}{2-q} \tag{16}$$

The quantity h/\mathcal{M}_q is particularly important from the experimental point of view, and is sketched in figure 5, for q<0.5 and $h = 3h_{0q}$.

Another interesting point of this model, for q < 0.5, is the existence of a *ferromagnetic phase transition induced by the magnetic field*, in the paramagnetic phase. In fact, sufficiently close to t_c , the two minima have similar free energy values and, consequently, the magnetic field energy plays a decisive role, being able to switch between the low and high magnetization values, inducing the first order phase transition. However, for sufficiently high temperatures $t \ge t_{0q}$, only one minimum exists for any value of magnetic field, and the phase transition becomes of second order character. This effect is illustrated in figure 6. The temperature t_{0q} , which determines the continuous or discontinuous nature of the magnetization versus field curve is given by:

$$t_{0q} = \frac{3(1-q)^2}{2-q} \tag{17}$$

Above t_{0q} , the magnetization as a function of magnetic field curves are continuous, presenting, however, a characteristic change of slope at such magnetic field h_c , which varies linearly with temperature, and is given by

$$h_c = \alpha(t - t') \tag{18}$$

where

$$t' = \frac{3q(1-q)}{(2-q)} \tag{19}$$

 and

$$\alpha = \frac{1}{1-q} \tag{20}$$

D. Magnetic Phase Diagrams

At this point it is convenient to summarize the main properties found so far: the behavior of the generalized magnetization and the generalized magnetic susceptibility with temperature and field depend greatly on the values assumed for the entropic parameter q. It can be the usual second order para-ferromagnetic phase transition but it can become first order, exhibiting the properties normally associated to this type of transitions.

Figure 7(a) presents the t-q phase diagram for several h values. The solid lines divide the plane in ferro (below) and paramagnetic (above) regions. For h = 0 and q > 0.5 the para-ferromagnetic phase transition is always second order, whereas for q < 0.5 the transition becomes first order. The dotted lines limit the stability regions of the fully ordered and disordered phases. In this way, the shaded area between such dotted lines represents the ferro-paramagnetic phase coexistence, which can exist for temperatures in the interval $t_{SC}(q) \leq t \leq t_{SH}(q)$.

Strictly, in the presence of the magnetic field h the ferro-paramagnetic phase transition does not exist for any temperature, since \mathcal{M}_q is always different from zero. In any case, for q < 0.5, if the magnetic field is not too high, the Gibbs free energy presents two minima close to t_c and we can always distinguish two phases, one with small magnetization \mathcal{M}_{a}^{small} and other with large magnetization \mathcal{M}_q^{large} . If the magnetic field is sufficiently high $h \ge h_{0q}$, the energy barrier disappears and the transition becomes continuous. However, in this case, the transition occurs with a characteristic slope change in magnetization versus temperature curves, which does not occur for q > 0.5. For q < 0.5 and up to a critical applied magnetic field, the phase transition occurs discontinuously, with the shaded areas corresponding to the values of temperature and q where phase coexistence occurs. The magnitude of the discontinuity $\Delta \mathcal{M}_q$ decreases with increasing field, disappearing for $h \ge h_{0q}$ (Eq.16), above which the transition is always second order (see figure 4). The dashed line cuts the transition lines at the point (q_{0h}, t_{0h}) , which divides each line into a first and second

order region. As the magnetic field increases, this points travels in the dashed curve according to the parametric equations:

$$q_{0h} = \frac{3-2h}{6-h}$$
(21)

$$t_{0h} = \frac{1}{3} \frac{(3+h)^2}{6-h} \tag{22}$$

In an analogous way, figure 7(b) presents the projection of the phase diagram in the h-q plane for several temperatures $t > t_c$. Each line divides the plane in the ferromagnetic region (above the curve) and in the paramagnetic region (below the curve). For q < 0.5 and sufficiently close to t_c , a field induced phase transition occurs discontinuously, with the dashed areas corresponding to the regions of phase coexistence. The magnitude of the discontinuity $\Delta \mathcal{M}_q$ decreases with increasing temperature, disappearing for $t \ge t_{0q}$ (Eq.17), above which the transition is always second order (see figure 6). The dashed line cuts the transition curves at the point (q_{0t}, h_{0t}) , which similarly as in the previous diagram, divides the curves in regions of first and second order phase transition. As the temperature increases, the point moves up along the curve according to the parametric equations given below, with corresponding increase of the second order region:

$$q_{0t} = \frac{6 - t - \sqrt{t^2 + 12t}}{6} \tag{23}$$

$$h_{0t} = \frac{6(t-3+\sqrt{t^2+12t})}{t+6+\sqrt{t^2+12t}}$$
(24)

The projection of the phase diagram in the h-t plane is presented in figure 7(c), only for q=0.1, for sake of clearness. Again, the dotted lines limit the stability regions of the para and ferromagnetic phases and the shaded area represents the values of field and temperature where the two phases can coexist. Above certain values of field and temperature h_{0q} and t_{0q} , the transition becomes second order and the characteristic field h_c varies linearly with temperature, as given by Eq.18. The open circle (t_{0q}, h_{0q}) divides the curve into the first and second order phase transition regions, and travels along the dashed curve according to Eqs.16 and 17.

E. Generalized Landau Coefficients

In this section we derive the generalized coefficients of Landau theory of phase transitions⁵⁵. Let us assume a reduced Gibbs free energy $\mathcal{G} = G/kT_C^{(1)}$, and magnetization $m = \mathcal{M}_q/\mu$. Thus, we are able to expand, for small values of magnetization, the previously presented Gibbs free energy (Eq.9), yielding:

$$\mathcal{G} = \frac{\mathcal{A}_q}{2}m^2 + \frac{\mathcal{B}_q}{4}m^4 + \frac{\mathcal{C}_q}{6}m^6 - hm \tag{25}$$

where,

$$\mathcal{A}_q = \frac{3}{q}(t-q) \tag{26}$$

$$\mathcal{B}_q = \frac{9(8q - 3 - 4q^2)t}{5q^3} \tag{27}$$

$$C_q = \frac{27(54 - 318q + 623q^2 - 464q^3 + 116q^4)t}{175q^5} \qquad (28)$$

Within the Landau theory, negative values of the coefficient \mathcal{B} mean first order transitions. In this direction, an obvious correlation between the model here proposed and the usual Landau theory is obtained, since for q < 1/2, the generalized Landau coefficient \mathcal{B}_q also assume negative values, as sketched in figure 8. Note that for q < 1/2our model also predicts first order transition. Additionally, still within the Landau theory, the parameter \mathcal{A} usually takes the form $\mathcal{A} = a(T - T_0)$ (Curie Law), and this is exactly the relation found for the generalized Landau coefficient \mathcal{A}_q (Eq.26 and sketched on the inset of figure 8), that represents the inverse of the generalized susceptibility (Eq.12).

It is well know^{56,57,58} that, using the classical formulation of the Landau theory, or similar, a negative slope of the isotherm plots h/m vs. m^2 (Arrot Plot) would indicate a first order phase transition. Thus, deriving the minimum of the Gibbs free energy $(d\mathcal{G}/dm = 0)$, we can express the h/m quantity as:

$$\frac{h}{m} = \mathcal{A}_q + \mathcal{B}_q m^2 + \mathcal{C}_q (m^2)^2 \tag{29}$$

As expected, for q < 1/2 the Generalized Arrot Plot has a negative slope, indicating first order transition, whereas for q > 1/2, these plots are straight lines, characteristic of a ferromagnetic second order phase transition. These features are presented in figure 9(a) and (b), for q > 1/2and q < 1/2, respectively.

IV. CONNECTIONS TO EXPERIMENTAL RESULTS

A. A Brief Survey

The experimental field and temperature dependencies of some manganites present interesting aspects. Mira *et al.*^{58,59} analyzed the character of the phase transition in $\text{La}_{2/3}(\text{Ca}_{1-y}\text{Sr}_y)_{1/3}\text{MnO}_3$ and concluded that for y=0 the magnetic transition is of first order, whereas it is second order for y=1. Other works, including those using nuclear magnetic resonance (NMR), support this result^{60,61}. Amaral *et al.*^{36,62,63} emphasized that $\text{La}_{0.67}\text{Ca}_{0.33}\text{MnO}_3$, $\text{La}_{0.8}\text{MnO}_3$ and $\text{La}_{0.60}\text{Y}_{0.07}\text{Ca}_{0.33}\text{MnO}_3$ exhibit first order transition

character, with additional hysteresis for fields below than a critical field $H < H_c^*$ and temperature ranges between T_C and a critical temperature T_C^* . For the last manganite cited above, for instance, M(H) presents an upward inflection point from $T_C=150$ K up to 220 K, with a characteristic field $H_c(T)$, for the inflexion point, presenting an almost liner temperature dependence. In addition, a large thermal hysteresis is clearly delimited for temperatures ranging from T_C up to the branching point $T_C^* \sim 170$ K. Analogous behavior are found in $La_{0.67}Ca_{0.33}MnO_3$ and $La_{0.8}MnO_3^{62}$, $Sm_{0.65}Sr_{0.35}MnO_3^{64}$ and $Pr_{0.5}Ca_{0.5}Mn_{0.95}Cr_{0.05}O_3^{65}$, among others.

Another interesting feature on the magnetization behavior of some manganites concerns the H/M vs T measurement, that presents a strong downturn for temperatures nearly above T_C . It makes a deviation from the simple Curie-Weiss law, and, at T_C , the magnetic state is quickly switched to a ferromagnetic one. Such feature is frequently found in the literature of manganites: $La_{0.60}Y_{0.07}Ca_{0.33}MnO_3$ and $La_{0.8}MnO_3^{63}$, $Sm_{0.55}Sr_{0.45}MnO_3^{66,67}$, $La_{0.825}Sr_{0.175}Mn_{0.86}Cu_{0.14}O_3^{68}$, $Ca_{1-x}Pr_xMnO_3$ with $x \leq 0.1^{69}$, among others.

However, even with the enormous quantity of experimental measurements on manganites (see, for example, the impressive review by Dagotto and co-workers⁴¹), the nature of the phase transition in ferromagnetic manganites is still a controversial issue. In this direction, Amaral *et al.*^{62,63} claim for new models to explain the first-second order character of the transition in manganites, even with the theoretical works developed by Jaime *et al.*⁷⁰, Alonso *et al.*⁷¹ and Novák *et al.*⁶⁰.

To inquire about the order of the phase transition and describe theoretically the behavior of the relevant magnetic quantities, Amaral and co-workers^{62,63} used the macroscopic Landau theory of phase transition, expanding the free energy up to sixth power of the magnetization. If the parameter \mathcal{B} (with respect to M^4) is negative, the transition can be first-order like. In this case, the magnetization will present large field cycling irreversibility only for fields and temperatures below H_c^* and T_C^* , respectively. Further analysis of Landau theory, even for $\mathcal{B} < 0$ and higher temperatures and magnetic fields (H>H $_{c}^{*}$ and T>T $_{C}^{*}$), show that the magnetization has a peculiar inflexion point at a characteristic magnetic field H_c , that increases linearly with temperature, $H_c(T) \propto (T-T_0)$. Mira *et al.*^{58,59} have also applied the Landau theory to manganites. However, the results of the Landau theory are not sufficient to reproduce all peculiar magnetic properties of the manganites, such as the anomalous behavior of the H/M vs. T quantity, presented on figure 5 and figure 12.

B. Experimental and theoretical results for $La_{0.60}Y_{0.07}Ca_{0.33}MnO_3$

A ferromagnetic ceramic $La_{0.60}Y_{0.07}Ca_{0.33}MnO_3$ was prepared by standard solid-state methods⁶³, and the magnetization was measured using a Quantum Design SQUID magnetometer (55 kOe) and an Oxford Instruments VSM (120 kOe).

In this section we will apply the general results obtained in the previous sections to a quantitative analysis of experimental data for $La_{0.60}Y_{0.07}Ca_{0.33}MnO_3$. As stated in section III, we work within the mean-field approximation, for which x assume the expression:

$$x = \frac{\mu(H + \lambda \mathcal{M}_q)}{kT} \tag{30}$$

where λ is the mean-field parameter. Figure 10 presents the measured and theoretical magnetic moment as a function of magnetic field, for several temperatures above T_C . The excellent experimental-theoretical agreement is due to the use of the Tsallis statistics, which parametrizes the system inhomogeneity⁴¹.

Here, we use q, μ , λ and N, the number of clusters in the sample, as free parameters. The magnetic moment μ of the clusters follows the usual temperature tendency of a para-ferromagnetic transition, whereas q increases towards unity with increasing temperature (figure 11). The temperature dependence of the q parameter was expected, since it should reach the unity for sufficiently high temperatures.

From these results, we were able to compare the anomalous downturn in H/M vs. T curves, just with the temperature dependence of q and μ , and the approximately constant values of λ and N. The calculated H/ \mathcal{M}_q vs. T curve is displayed in figure 12, with its corresponding experimental value. One should stress that the solid line in this plot does not include any other fitting parameter. The curve was calculated using only the fitted parameters obtained from Figure 10.

Additionally, Amaral and co-workers pointed out that $La_{0.60}Y_{0.07}Ca_{0.33}MnO_3^{62}$ presents two different features on the inflection point, at H_c , of its M vs. H curves: (i) a linear temperature dependence of the characteristic field H_c , for $T>T_C^*$, and (ii) an observed hysteresis for temperatures in the range $T_C < T < T_C^*$. Figure 13 shows the plot of H_c vs. T obtained from experimental data. It is striking the similarity between this plot and the curve shown in Fig. 7(c).

Finally, the Arrot Plots presented by Amaral *et al.*^{62,63} and Mira *et al.*^{58,59} are very similar to those presented on figure 9(a)(b).

V. CONCLUSION

In two previous publications^{34,35} we presented evidences that the magnetic properties of manganites can be suitably described in the framework of Tsallis statistics. In the present paper we have extended our analysis and presented new compelling evidences in this direction by deducing a magnetic phase diagram which matches observed experimental results on La_{0.60}Y_{0.07}Ca_{0.33}MnO₃, along with some other magnetic properties of this compound. The interpretation of the entropic parameter q, given by Beck and Cohen⁴⁹, in terms of the ratio between the mean and width of the temperature distribution in the system, comes to support our proposal, since manganites have long been recognized as objects whose properties are dominated by intrinsic inhomogeneities^{41,50,66}. Such a distribution can be translated as a distribution of the magnetic susceptibility, as pointed out by Salamon et $al.^{51}$, from which a temperature dependence of q can be expected. Therefore, we conclude that the Tsallis nonextensive statistics is a handy tool to study, classify and predict magnetic and thermal properties of manganites.

VI. ACKNOWLEDGEMENTS

The authors thanks FAPERJ/Brasil, FCT/Portugal (contract POCTI/CTM/35462/99) and ICCTI/CAPES (Portugal-Brasil bilateral cooperation), for financial support. We are also thankful to A.P. Guimarães, E.K. Lenzi and R.S. Mendes, for their helpful suggestions.

VII. FIGURE CAPTIONS

Figure 1. Gibbs free energy(Eq.9), within the mean field approximation and h = 0, as a function of the reduced magnetization. (a) For q > 0.5 only one minimum is observed, for any value of temperature $(t>t_c \text{ or } t<t_c)$, representing a second order phase transition for the magnetization. (b) For q < 0.5 and $t=t_c$ two degenerated minima are observed, representing a first order phase transition. The t_{SH} and t_{SC} temperatures limit the 'superheating' and 'supercooling' cycle, responsible for the thermal hysteresis normally observed in first order transitions.

Figure 2. Temperature dependence of the reduced equilibrium magnetization for several values of q and h = 0. For q < 1/2 the transition shows a first order character, whereas for q > 1/2 the transition is of second order type. Inset: Thermal hysteresis normally observed in first order phase transitions, with the 'superheating' and 'supercooling' cycles.

Figure 3. Temperature dependence of the generalized magnetic susceptibility χ_q , and its inverse, for (a) q < 0.5 and (b) q > 0.5.

Figure 4. Temperature dependence of the reduced equilibrium magnetization for several values of h, and q = 0.1. Sufficiently high magnetic field $h \ge h_{0q}$ (Eq.16), is able to remove the discontinuity in the equilibrium magnetization curve.

Figure 5. Temperature dependence of the quantity h/M_q , for q = 0.2 and $h = 3h_{0q}$.

Figure 6. Magnetic field dependence of the reduced equilibrium magnetization for several values of temperature, and q = 0.1. It represents a genuine ferromagnetic phase transition induced by magnetic field, in the paramagnetic phase. For sufficiently high temperatures $t \ge t_{0q}$ (Eq.17), the transition becomes continuous. Figure 7. q-magnetic phase diagram summarizing the main properties found in the model. (a) Projection of the phase diagram in t-q plane. The solid lines divide the plane in ferro (below) and paramagnetic (above) phases, with a region of phase coexistence between the dotted lines (shaded area). On the left side of the dashed line, the transition has a first order character, whereas a second order character arises for the right side. (b) Projection of the phase diagram in h-q plane, for several temperatures $t>t_c$. The curves in this case have a complete analogy to the previous one, however, it is ferromagnetic transition induced by magnetic field. (c) Projection of the phase diagram in the h-t plane, for q = 0.1. Above certain values of field and temperatures h_{0q} (Eq.17), the transition becomes second order.

Figure 8. The generalized Landau coefficient \mathcal{B}_q as a function of the entropic parameter q. For q < 0.5, \mathcal{B}_q assume negative values, indicating first order phase transition. Inset: temperature dependence of the parameter \mathcal{A}_q , that represents the inverse of the generalized susceptibility.

- * Present address: Centro Brasileiro de Pesquisas Físicas, Rua Dr. Xavier Sigaud 150 Urca, 22290-180 Rio de Janeiro-RJ, Brasil; Electronic address: marior@fis.ua.pt
- ¹ V. N. Krivoruchko, S. I. Khartsev, A. D. Prokhorov, V. I. Kamenev, R. Szymczak, M. Baran, and M. Berkowski, J. Magn. Magn. Mater. **207**, 168 (1999).
- ² J. E. Nunez-Regueiro and A. M. Kadin, Appl. Phys. Lett. **68**, 2747 (1996).
- ³ G. F. Dionne, J. Appl. Phys. **79**, 5172 (1996).
- ⁴ V. Ravindranath, M. S. Ramachandra, G. Rangarajan, L. Yafeng, J. Klein, R. Klingeler, S. Uhlenbruck, B. Büchner, and R. Gross, Phys. Rev. B 63, 184434 (2001).
- ⁵ J. Rivas, L. E. Hueso, A. Fondado, F. Rivadulla, and M. A. López-Quintela, J. Magn. Magn. Mater. **221**, 57 (2000).
- ⁶ L. E. Hueso, F. Rivadulla, R. D. Sánchez, D. Caeiro, C. Jardón, C. Vázquez-Vázquez, J. Rivas, and M. A. López-Quintela, J. Magn. Magn. Mater. **189**, 321 (1998).
- ⁷ J. J. Heremans, M. Carris, S. Watts, X. Yu, K. H. Dahmen, and S. von Molnár, J. Appl. Phys. 81, 4967 (1997).
- ⁸ S. Pal, A. Banerjee, E. Rozenberg, and B. K. Chaudhuri, J. Appl. Phys. **89**, 4955 (2001).
- ⁹ J. Philip and T. R. N. Kutty, J. Phys. Condens. Matter 11, 8537 (1999).
- ¹⁰ A. Szewczyk, H. Szymczac, A. Wisniewski, K. Piotrowski, R. Kartaszynski, B. Dabrowski, S. Kolesnik, and Z. Bukowski, Appl. Phys. Lett. **77**, 1026 (2000).
- ¹¹ M. Viret, L. Ranno, and J. M. D. Coey, Phys. Rev. B **55**, 8067 (1997).
- ¹² A. Tkachuk, K. Rogackia, D. E. Brown, B. Dabrowski, A. J. Fedro, C. W. Kimball, B. Pyles, X. Xiong, D. Rosenmann, and B. D. Dunlap, Phys. Rev. B 57, 8509 (1998).
- ¹³ C. Tsallis, J. Stat. Phys. **52**, 479 (1988).
- ¹⁴ C. Tsallis, R. S. Mendes, and A. R. Plastino, Physica A 261, 534 (1998).
- ¹⁵ C. Tsallis, Nonextensive Statistical Mechanics and Its Applications (Springer-Verlag, Heidelberg, 2001), chap. Nonextensive Statistical Mechanics and Thermodynamics: Historical Background and Present Status, eds. S. Abe and Y. Okamoto.

Figure 9. The generalized Arrot Plot (h/m vs. m^2 curves), for (a) q > 0.5 and (b) q < 0.5.

Figure 10. Measured (open circles) and theoretical (solid lines - Eqs.7 and 30) magnetic moment as a function of magnetic field, for several values of temperatures above $T_C=150$ K.

Figure 11. Temperature dependence of the fitting parameters, q and μ (see text).

Figure 12. Measured (open circles) and theoretical (solid lines) values of the quantity H/M vs. T. The solid line in this plot does not include any fitting parameters, and was calculated using only the fitted parameters obtained from figure 10.

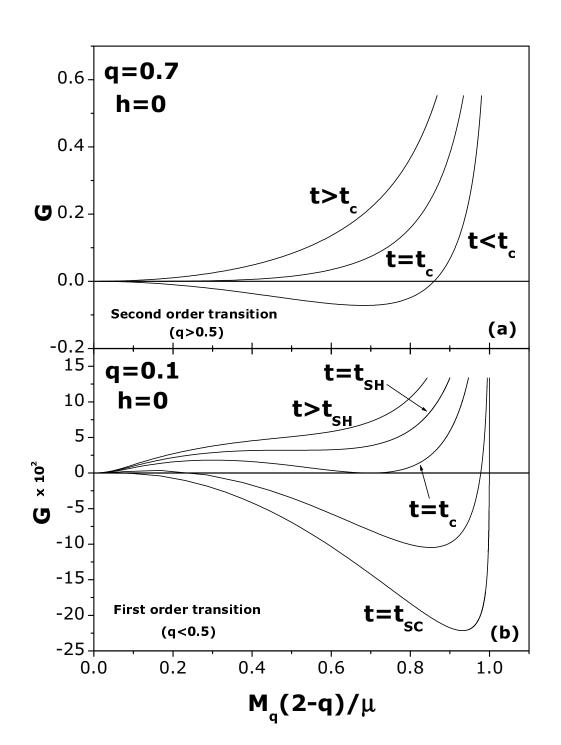
Figure 13. The linear temperature dependence, for $T>T_C^*$, of the characteristic field H_c , which corresponds to the inflexion point of the experimental M vs. H curves, measured in La_{0.60}Y_{0.07}Ca_{0.33}MnO₃. For $T_C < T < T_C^*$ the hysteresis is indicated by the shaded area. It is striking the similarity between this experimental plot and the theoretical one, shown in figure 7(c).

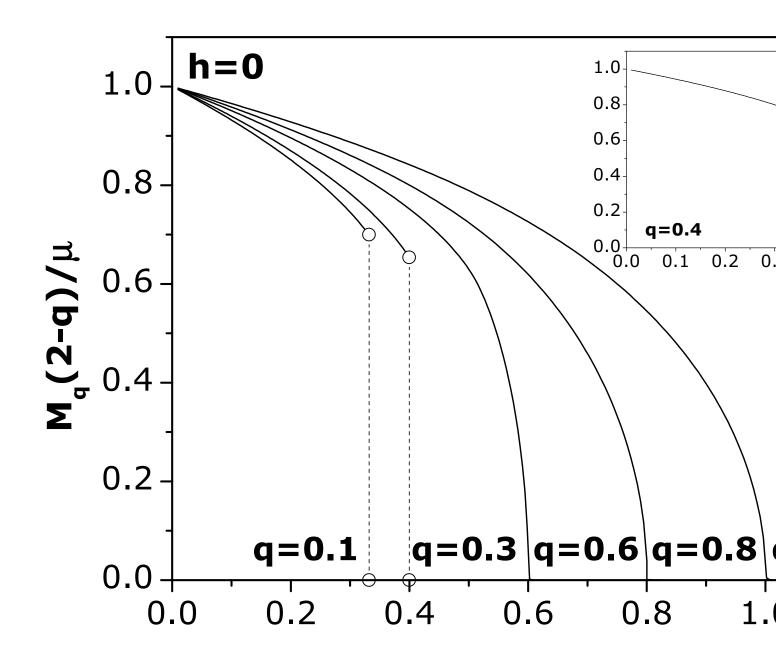
- ¹⁶ C. Tsallis, Braz. J. Phys. **29**, 1 (1999).
- ¹⁷ For a complete and updated list of references, see the web site: tsallis.cat.cbpf.br/biblio.htm.
- ¹⁸ R. F. S. Andrade, Physica A **175**, 285 (1991).
- ¹⁹ R. F. S. Andrade, Physica A **203**, 486 (1994).
- ²⁰ U. Tirnakli, D. Demirhan, and F. Buyukkilić, Acta Phys. Polonica A **91**, 1035 (1997).
- ²¹ S. A. Cannas and A. C. N. Magalhães, J. Phys. A **30**, 3345 (1997).
- ²² L. C. Sampaio, M. P. Albuquerque, and F. S. Menezes, Phys. Rev. B 55, 5611 (1997).
- ²³ F. Buyukkilic, U. Tirnakli, and D. Demirhan, Tr. J. Phys. (Turkey) **21**, 132 (1997).
- ²⁴ S. A. Cannas, A. C. N. Magalhaes, and F. A. Tamarit, Phys. Rev. B **61**, 11521 (2000).
- ²⁵ F. Buyukkilic, D. Demirhan, and U. Tirnakli, Physica A 238, 285 (1997).
- ²⁶ H. H. A. Rego, L. S. Lucena, L. R. Silva, and C. Tsallis, Physica A **266**, 42 (1999).
- ²⁷ S. F. Ozeren, U. Tirnakli, F. Buyukkilic, and D. Demirhan, Eur. Phys. J. B 2, 101 (1998).
- ²⁸ U. Tirnakli, S. F. Özeren, F. Buyukkilic, and D. Demirhan, Z. Physik B **104**, 341 (1997).
- ²⁹ I. Koponen, Phys. Rev. E **55**, 7759 (1997).
- ³⁰ H. N. Nazareno and P. E. Brito, Phys. Rev. B **60**, 4629 (1999).
- ³¹ L. Borland and J. G. Menchero, Braz. J. Phys. 29, 169 (1999).
- ³² I. S. Óliveira, Eur. Phys. J. B **14**, 43 (2000).
- ³³ L. H. C. M. Nunes and E. V. L. Mello, Physica A **296**, 106 (2001).
- ³⁴ M. S. Reis, J. C. C. Freitas, M. T. D. Orlando, E. K. Lenzi, and I. S. Oliveira, Europhys. Lett. 58, 42 (2002).
- ³⁵ M. S. Reis, J. P. Araújo, V. S. Amaral, E. K. Lenzi, and I. S. Oliveira, Phys. Rev. B 66, 134417 (2002).
- ³⁶ V. S. Amaral, J. P. Araújo, Y. G. Pogorelov, J. M. B. L. dos Santos, P. B. Tavares, A. A. C. S. Lourenço, J. B. Sousa, and J. M. Vieira, J. Magn. Magn. Mater. **226**, 837 (2001).

- ³⁷ A. K. Rajagopal, Nonextensive Statistical Mechanics and Its Applications (Springer-Verlag, Heidelberg, 2001), chap. Quantum Density Matrix Description of Nonextensive Systems, eds. S. Abe and Y. Okamoto.
- ³⁸ S. Abe, S. Martinez, F. Pennini, and A. Plastino, Phys. Lett. A **281**, 126 (2001).
- ³⁹ S. Abe, Physica A **300**, 417 (2001).
- ⁴⁰ A. K. Rajagopal and S. Abe, Phys. Rev. Lett. 83, 1711 (1999).
- ⁴¹ E. Dagotto, T. Hotta, and A. Moreo, Phys. Rep. **344**, 1 (2001).
- ⁴² M. Mayr, A. Moreo, J. A. Vergés, J. Arispe, A. Feiguin, and E. Dagotto, Phys. Rev. Lett. 86, 135 (2001).
- ⁴³ A. L. Malvezzi, S. Yunoki, and E. Dagotto, Phys. Rev. B 59, 7033 (1999).
- ⁴⁴ A. Moreo, S. Yunoki, and E. Dagotto, Science **283**, 2034 (1999).
- ⁴⁵ J. Lorenzana, C. Castellani, and C. D. Castro, Phys. Rev. B 64, 235127 (2001).
- ⁴⁶ R. D. Merithew, M. B. Weissman, F. M. Hess, P. Spradling, E. R. Nowak, J. O'Donnell, J. N. Eckstein, Y. Tokura, and Y. Tomioka, Phys. Rev. Lett. **84**, 3442 (2000).
- ⁴⁷ M. Fiebig, K. Miyano, Y. Tomioka, and Y. Tokura, Science 280, 1925 (1998).
- ⁴⁸ A. Satou and M. Yamanada, Phys. Rev. B **63**, 212403 (2001).
- ⁴⁹ C. Beck and E. G. D. Cohen, cond-mat/0205097.
- ⁵⁰ M. S. Reis, V. S. Amaral, P. B. Tavares, A. M. Gomes, A. Y. Takeuchi, A. P. Guimarães, I. S. Oliveira and P. Panissod, cond-mat/0211143.
- ⁵¹ M. B. Salamon, P. Lin, and S. H. Chun, Phys. Rev. Lett. 88, 197203 (2002).
- ⁵² E. P. Borges, J. Phys. A: Math. Gen. **31**, 5281 (1998).
- ⁵³ A. R. Lima and T. J. P. Penna, Phys. Lett. A 256, 221 (1999).
- ⁵⁴ A. Plastino and A. R. Plastino, Braz. J. Phys. **29**, 50 (1999).
- ⁵⁵ D. I. Uzinov, Introduction to the Theory of Critical Phe-

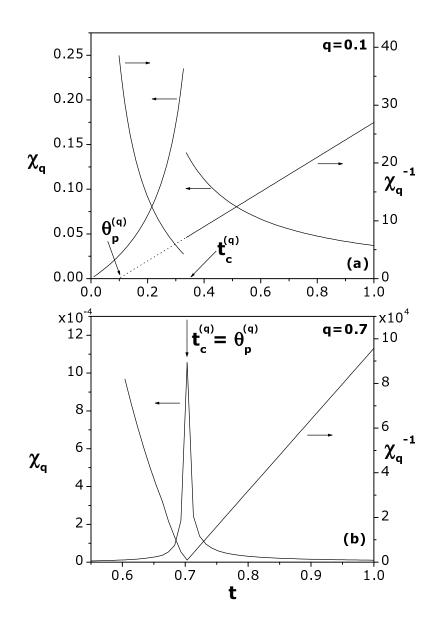
nomena (World Scientific, Singapore, 1993).

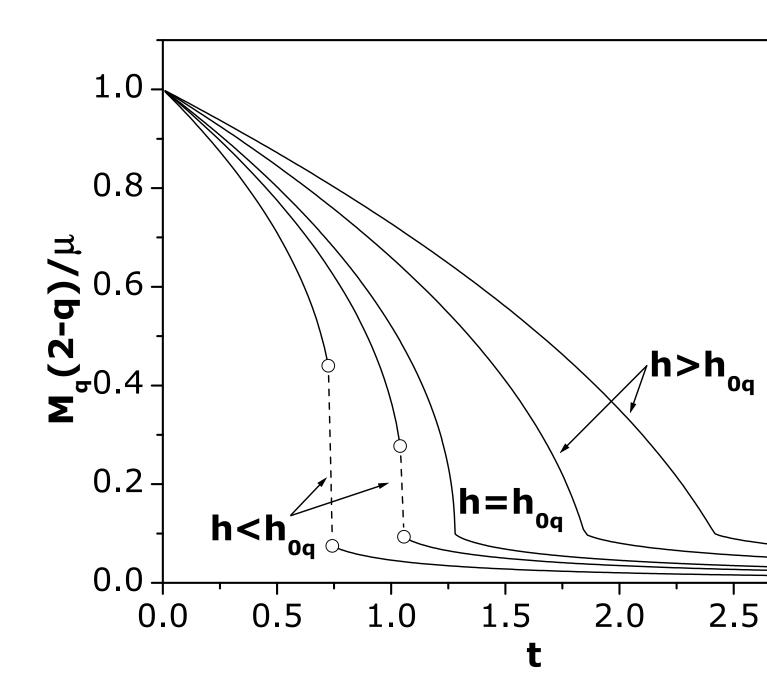
- ⁵⁶ C. P. Bean and D. S. Rodbell, Phys. Rev. **126**, 104 (1962).
- ⁵⁷ S. K. Banerjee, Phys. Lett. **12**, 16 (1964).
- ⁵⁸ J. Mira, J. Rivas, F. Rivadulla, and M. A. L. Quintela, Physica B **320**, 23 (2002).
- ⁵⁹ J. Mira, J. Rivas, F. Rivadulla, C. Vázquez-Vázquez, and M. A. López-Quintela, Phys. Rev. B **60**, 2998 (1999).
- ⁶⁰ P. Novák, M. Marysko, M. M. Savosta, and A. N. Ulyanov, Phys. Rev. B **60**, 6655 (1999).
- ⁶¹ Y. Tomioka, A. Asamitsu, and Y. Tokura, Phys. Rev. B 63, 024421 (2000).
- ⁶² V. S. Amaral, J. P. Araújo, Yu. G. Pogorelov, J. B. Sousa, P. B. Tavares, J. M. Vieira, P. A. Algarabel and M. R. Ibarra, to appear in J. Appl. Phys.
- ⁶³ V. S. Amaral, J. P. Araújo, Y. G. Pogorelov, P. B. Tavares, J. B. Sousa, and J. M. Vieira, J. Magn. Magn. Mater. **242**, 655 (2002).
- ⁶⁴ R. P. Borges, F. Ott, R. M. Thomas, V. Skumryev, and J. M. D. Coey, Phys. Rev. B **60**, 12847 (1999).
- ⁶⁵ R. Mahendiran, M. Hervieu, A. Maignan, C. Martin, and B. Raveau, Solid State Commun. **114**, 429 (2000).
- ⁶⁶ Y. Tokura and Y. Tomioka, J. Magn. Magn. Mater. **200**, 1 (1999).
- ⁶⁷ J. M. D. Teresa, M. R. Ibarra, P. Algarabel, L. Morellon, B. Gracia-Landa, C. Marquina, C. Ritter, A. Maignan, C. Martin, B. Raveau, et al., Phys. Rev. B **65**, 100403 (2002).
- ⁶⁸ L. Zheng, X. Xu, L. Pi, and Y. Zhang, Phys. Rev. B 62, 1193 (2000).
- ⁶⁹ M. M. Savosta, P. Novak, M. Marysko, Z. Jirk, J. Hejtmanek, J. Englich, J. Kohout, C. Martin, and B. Raveau, Phys. Rev. B **62**, 9532 (2000).
- ⁷⁰ M. Jaime, P. Lin, S. H. Chun, M. B. Salamon, P. Dorsey, and M. Rubinstein, Phys. Rev. B **60**, 1028 (1999).
- ⁷¹ J. L. Alonso, L. A. Fernandez, F. Guinea, V. Laliena, and V. Martin-Mayor, Phys. Rev. B 63, 054411 (2001).

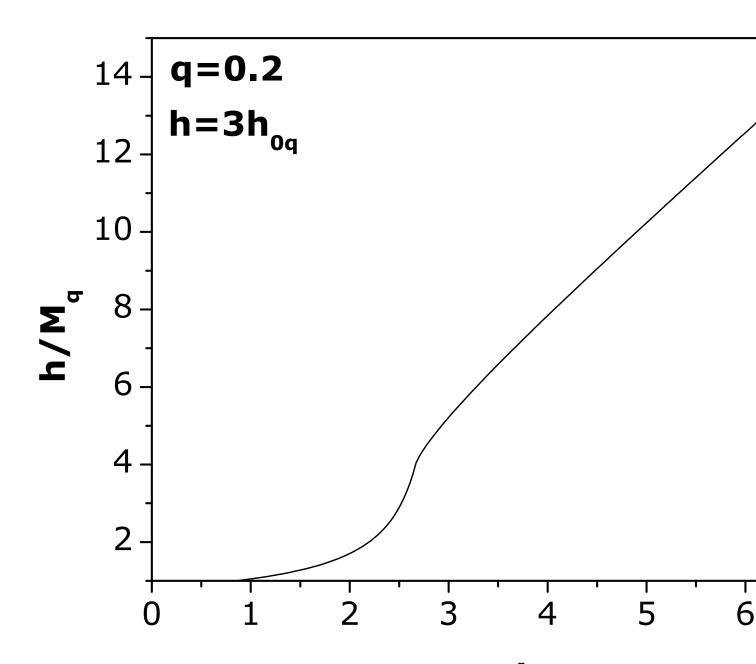




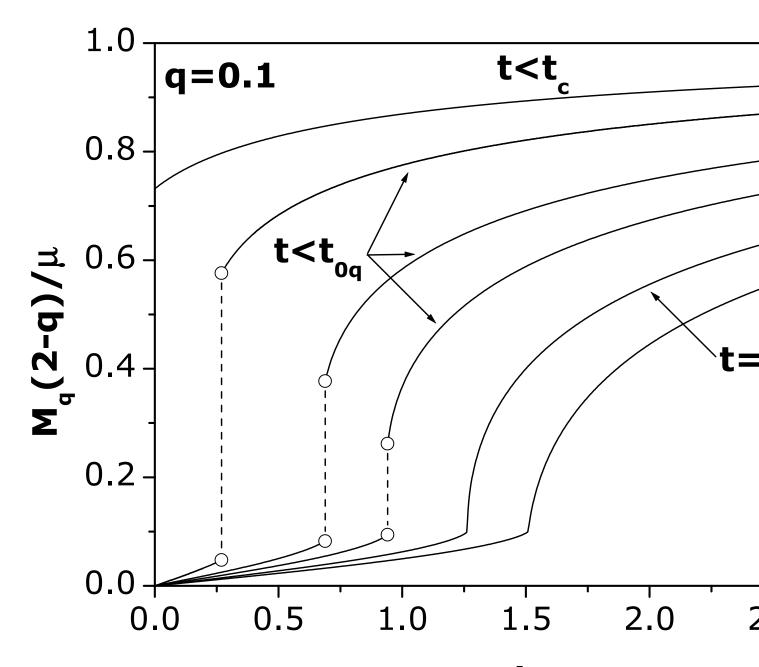
t







t



h

